

UDK 676.017.5; 625.074

## Effect of Electrodeposition Current Density on the Microstructure and Magnetic Properties of Nickel-cobalt-molybdenum Alloy Powders

O. Pešić<sup>1</sup>, M. Spasojević<sup>1,2\*)</sup>, B. Jordović<sup>1</sup>, P. Spasojević<sup>1,3</sup>, A. Maričić<sup>1</sup>

<sup>1</sup>Joint Laboratory for Advanced Materials of SASA, Section for Amorphous Systems Technical Faculty, Čačak, Svetog Save 65, Serbia

<sup>2</sup>Faculty of Agronomy, University of Kragujevac, Čačak, Cara Dušana 34, Serbia

<sup>3</sup>Faculty of Technology and Metallurgy, University of Belgrade, Belgrade, Karnegijeva 4, Serbia

---

### Abstract:

*Nanostructured nickel-cobalt-molybdenum alloy powders were electrodeposited from an ammonium sulfate bath. The powders mostly consist of an amorphous phase and a very small amount of nanocrystals with a mean size of less than 3 nm. An increase in deposition current density increases the amorphous phase percentage, the density of chaotically distributed dislocations and internal microstrains in the powders, while decreasing the mean nanocrystal size. The temperature range over which the structural relaxation of the powders deposited at higher current densities occurs is shifted towards lower temperatures. A change in relative magnetic permeability during structural relaxation is higher in powders deposited at higher current densities. Powder crystallization takes place at temperatures above 700°C. The formation of the stable crystal structure causes a decrease in relative magnetic permeability.*

**Keywords:** X-ray diffraction, Nanostructured materials, Dislocations, Magnetic permeability, Powder.

---

## 1. Introduction

Nanostructured metallic alloys have been extensively used in electrical engineering, electronics and other industries due to their specific physical and chemical properties [1-4]. Nanostructured powders of metallic alloys have also found wide application in modern technologies [5-7].

Nanostructured nickel-cobalt alloys exhibit good electrical and magnetic properties [9-24]. Small additions of molybdenum to these alloys improve their corrosion resistance, thermal stability and mechanical properties [15,16,24-29].

The metallurgic production of nanostructured nickel-cobalt-molybdenum alloy powders is a rather expensive process due to high energy consumption. Therefore, the development of electrochemical procedures for the fabrication of amorphous alloys has recently been the focus of many studies [9-29]. The properties of electrochemically obtained powders are often quite different from those of the powders of the same chemical composition

---

\*) Corresponding author: mspasojevic@kg.ac.rs

produced by other methods[9-35]. Chemical and physical properties of electrochemically obtained alloys are dependent on kinetic and operating electrolysis parameters.

Pure molybdenum cannot be obtained by electrolysis from aqueous solutions. However, it can be codeposited along with iron-group metals [15,16,24-29,36-39]. A number of studies explaining the kinetics and mechanism of codeposition of molybdenum and iron-group metals have been published [15,16,24-29,36-39].

Effects of current density and solution composition, temperature and pH on the chemical composition, phase structure, mechanical, electrical and magnetic properties, corrosion and wear resistance and thermal stability of electrodeposited nickel-cobalt-molybdenum alloys have been reported [15,16,24-29,36-39].

Amorphous alloys exhibit a metastable structure. Annealing at temperatures below the crystallization temperature results in structural relaxation in these alloys [14-18,25-29,40-42]. Structural changes occurring during relaxation and crystallization lead to changes in the mechanical, electrical, magnetic and chemical properties of these alloys.

The objective of this study was to evaluate the effect of electrodeposition current density on the chemical composition, microstructure and magnetic properties of nickel-cobalt-molybdenum alloy powders obtained from an ammonium sulfate bath. Moreover, the effect of annealing temperature on the microstructure and magnetic properties of the alloys was also dealt with in this research.

## 2. Experimental

Nickel-cobalt-molybdenum alloy powder was deposited from an ammonium sulfate bath onto a titanium cathode. The composition of the electrolyte solution was as follows:  $0.176 \text{ mol dm}^{-3} \text{ NiSO}_4$ ;  $0.044 \text{ mol dm}^{-3} \text{ CoSO}_4$ ;  $0.035 \text{ mol dm}^{-3} (\text{NH}_4)_6\text{Mo}_7\text{O}_{24}$ ;  $0.53 \text{ mol dm}^{-3} \text{ NH}_4\text{Cl}$ . The temperature and pH of the solution during the electrolysis were  $22 \pm 2^\circ\text{C}$  and  $10.6 \pm 0.1$ , respectively. The pH of the solution was adjusted by addition of  $0.6 \text{ mol dm}^{-3} \text{ NH}_4\text{OH}$ . The solution was prepared using analytical grade chemicals and double-distilled water. The volume of the electrolyzer was  $5.5 \text{ dm}^3$ . The anode was a  $100 \text{ cm}^2 \text{ Pb/PbO}_2$  plate. A  $32 \text{ cm}^2$  plate-shaped titanium cathode was positioned parallel to the anode. During the electrolysis, a standard electrical circuit comprising an automatic rectifier and ammeter was used. Powders were deposited under galvanostatic conditions at current densities of 400; 800 and  $1600 \text{ mAcm}^{-2}$ . Upon electrolysis, the powders were washed with distilled water and, then, with 0.1 wt.% benzoic acid solution.

The chemical composition of the powders was determined by energy dispersive X-ray spectroscopy (EDS) (JEOL-JSM 5300 equipped with an EDS-QX 3000 spectrometer) as well as by atomic absorption (PEKTAR-A A 200-VARIAN).

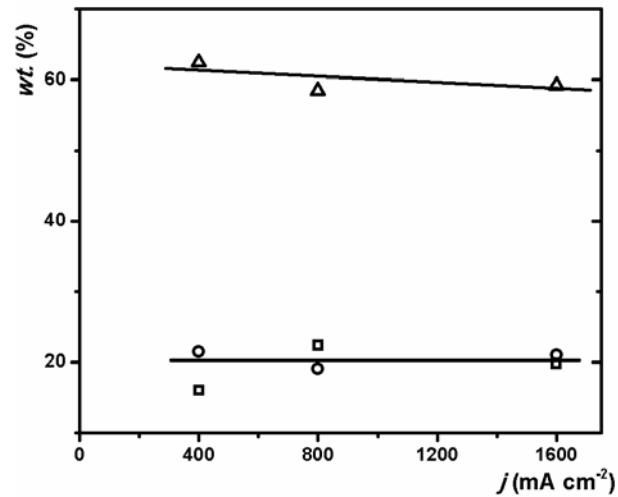
X-ray diffraction (XRD) was recorded on a Philips PW 1710 diffractometer using  $\text{CuK}_\alpha$  radiation ( $\lambda=0.154 \text{ nm}$ ) and a graphite monochromator. XRD data were collected with a step mode of  $0.03^\circ$  and collection time of  $1.5 \text{ s step}^{-1}$ .

Magnetization measurements were performed using a modified Maxwell method, based on the action of an inhomogeneous field on the magnetic sample. Magnetic force measurements were performed with a sensitivity of  $10^{-6} \text{ N}$  in an argon atmosphere.

## 3. Results and discussion

Nickel-cobalt-molybdenum alloy powders were deposited from an ammonium sulfate bath onto a titanium cathode at current densities of 400, 800 and  $1600 \text{ mAcm}^{-2}$ . The chemical composition of the powders was determined by both atomic absorption and EDS analysis.

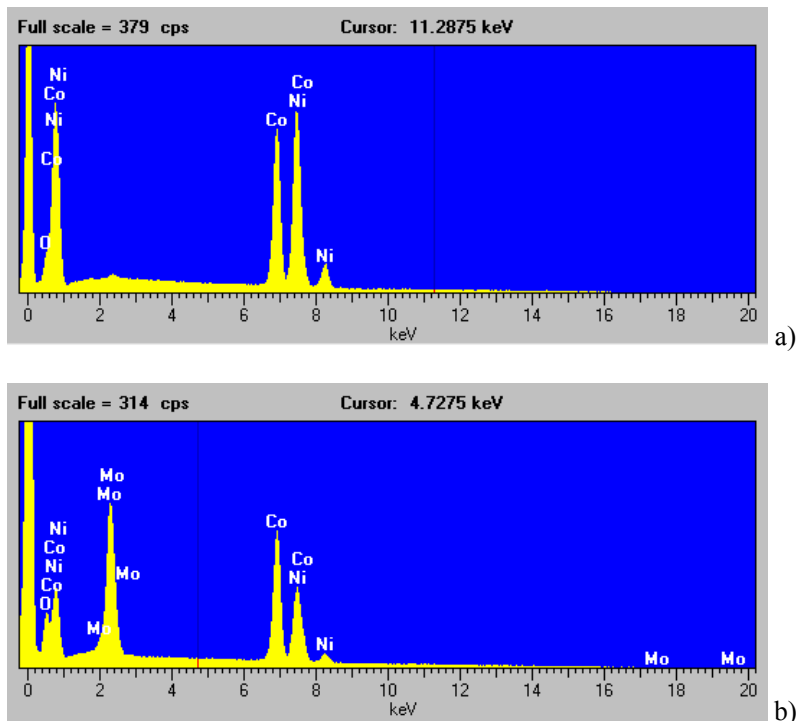
Three atomic absorption measurements were performed per sample to evaluate the average chemical composition. The values obtained are presented in Fig. 1.



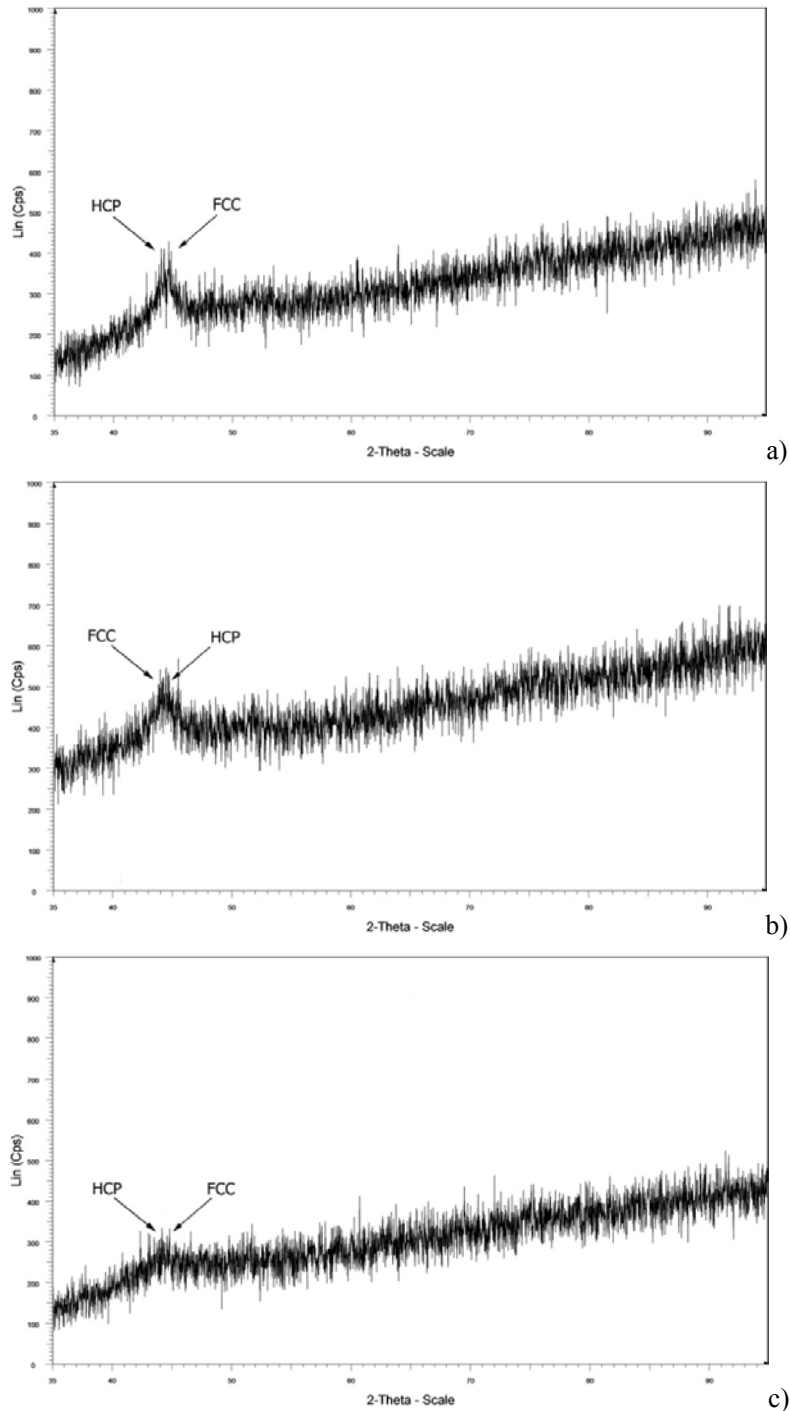
**Fig. 1.** Composition of powders obtained at different cathodic current densities: o - Mo;  $\Delta$  - Ni;  $\square$  - Co.

Fig. 1 shows that the chemical composition of the powders obtained in the current density range of 400 to 1600 mAcm<sup>-2</sup> practically does not depend on current density, suggesting that the three metals are codeposited under limiting currents.

EDS spectra (Fig. 2) for the samples obtained at the three current densities show that all three powders have non-homogeneous composition and an oxygen content of about 8 wt.%.



**Fig. 2.** EDS spectra for the sample of the powder obtained at 800 mAcm<sup>-2</sup>.



**Fig. 3.** X-ray diffractograms for the as-deposited powders obtained at current densities: a) –  $400 \text{ mAcm}^{-2}$ ; b) –  $800 \text{ mAcm}^{-2}$ ; c) –  $1600 \text{ mAcm}^{-2}$ .

Oxygen is most likely present on the powder surface in the form of oxides or hydroxides of the metals. XRD analysis revealed that the electrochemically obtained nickel and molybdenum alloy powders contain nickel and molybdenum oxides in the surface layer.

M. Donten [43] also showed that the electrodeposited alloys of iron-group metals and tungsten do not contain oxygen in the alloy bulk. The presence of oxygen in the form of oxides was found only in the thin surface layer. It was assumed that these oxides are the result of oxidation of the alloy under atmospheric oxygen. Small amounts of nickel and cobalt hydroxides may form in the alkaline environment to become, thereafter, present as inclusions in the deposit.

XRD analysis was used to determine the phase structure of the powders (Fig. 3).

XRD patterns show that nickel-cobalt-molybdenum alloy powders deposited from ammonium sulfate bath in the current density range of 400 to 1600 mAcm<sup>-2</sup> mostly consist of an amorphous phase. In the X-ray diffractograms for all three powders (Fig. 3) at 43° < 2θ < 46° two weak overlapping peaks are observed, indicating that these powders also contain a very small amount of the FCC phase of the solid solution of cobalt and molybdenum in nickel and the HCP phase of the solid solution of nickel and molybdenum in cobalt with an average crystal grain size of about 3 nm.

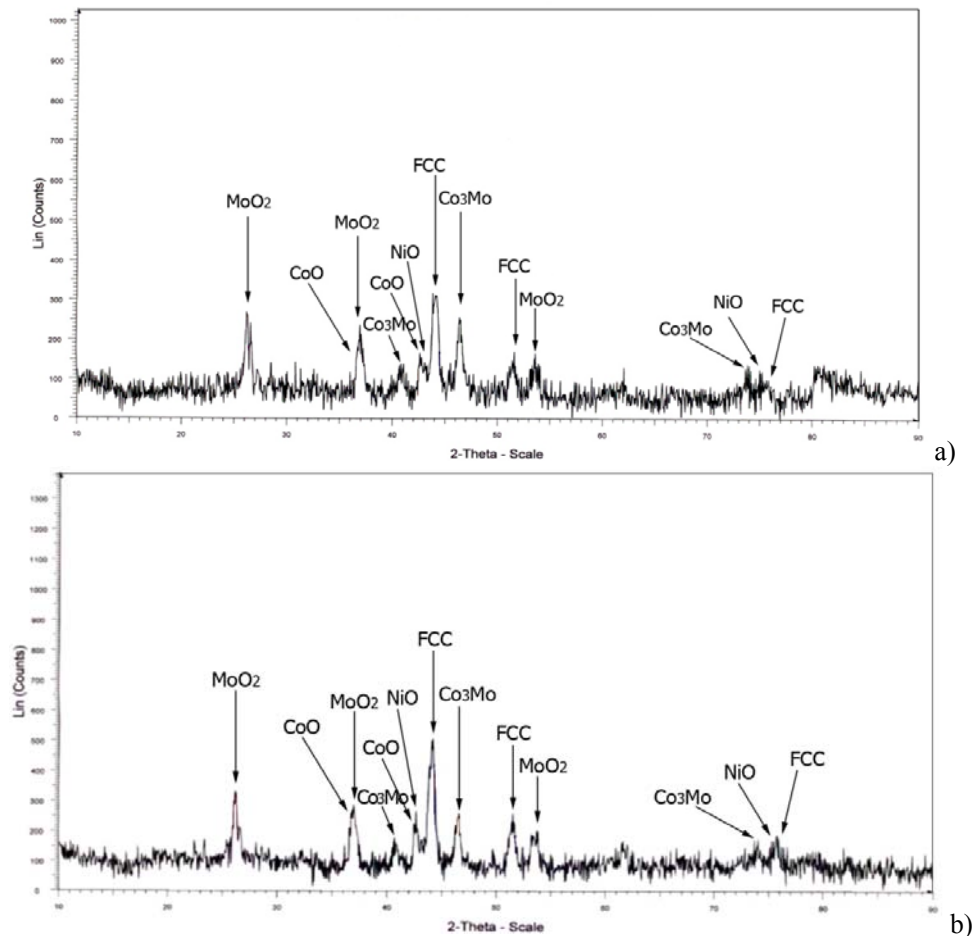


**Fig. 4.** X-ray diffractograms for the powders annealed at 700 °C, obtained at current densities of a) – 400 mAcm<sup>-2</sup> and b) – 800 mAcm<sup>-2</sup>.

It is well known that at current densities below 400 mAcm<sup>-2</sup> deposits containing considerably larger crystal grains of the FCC and HCP phases of solid solutions are produced from an ammonium sulfate bath having a lower molybdate content [24-29]. However, high overvoltages, a high electrodeposition current density and a high molybdenum content in the

alloy cause the formation of an amorphous phase [24-29]. The small value of the relative integrated intensities of the peaks at  $43^\circ < 2\theta < 46^\circ$  confirms that the powders mostly consist of the amorphous phase. An increase in deposition current density decreases the relative integrated intensities of the peaks, suggesting that the powders obtained at higher current densities have a higher content of the amorphous phase. The FCC and HCP crystal grains formed at higher current densities have a lower average size value. EDS spectra for the powders show that the high current density during nickel-cobalt-molybdenum alloy deposition causes chemical composition inhomogeneity of the amorphous phase.

The as-deposited powders were annealed for 30 minutes at 550, 650 and 700°C. Then, they were cooled to 25°C. Their XRD patterns were recorded thereafter. XRD patterns of the powders annealed at 550 and 650°C were found to match those of the as-deposited powders. This suggests that amorphous phase crystallization does not take place at annealing temperatures below 650 °C.

XRD diffractograms for the powders annealed at 700 °C show the existence of peaks characterizing the presence of the FCC phase of the solid solution of cobalt and molybdenum in nickel, the oxide phase of molybdenum,  $\text{MoO}_2$ , cobalt  $\text{CoO}$  and nickel,  $\text{NiO}$ , and the intermetallic compound  $\text{Co}_3\text{Mo}$  phase (Fig. 4).

Thus, annealing at 700°C results in the following: amorphous phase crystallization, FCC crystal grain growth, HCP-FCC phase transformation, formation of oxides of all three metals, and the formation of the intermetallic compound,  $\text{Co}_3\text{Mo}$ . Metal oxides are produced through the reaction of the metals with the small amount of oxygen present in the argon. The ratio of the relative integrated peak intensity in the diffractogram of the annealed powder to that of the as-deposited powder suggests that the as-deposited powder contains over 90% of the amorphous phase. FCC phase peaks are shifted towards lower  $2\theta$  values relative to the position of the peaks of the pure nickel FCC phase. The shift in the peak maximum indicates the presence of molybdenum in the FCC phase. Molybdenum causes deformation to the crystal lattice of the nickel FCC phase since it increases the mean interatom distance. The results presented show that the microstructure of the electrodeposited nickel-cobalt-molybdenum alloy powders is dependent on deposition current density and annealing temperature. Magnetic properties are governed by the microstructure [14-18,25-29].

Fig. 5. shows the relative change in the magnetic permeability of the powder deposited at  $400 \text{ mAcm}^{-2}$  as a function of temperature.

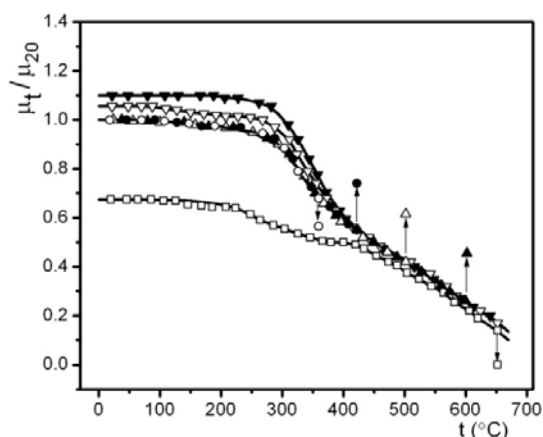


**Fig. 5.** Relative change in the magnetic permeability of the powder deposited at  $400 \text{ mAcm}^{-2}$  as a function of temperature: o – first heating to 360°C; ● – second heating to 420 °C; Δ - third heating to 500 °C; ▲ – fourth heating to 600 °C; ◀ – fifth heating to 650 °C; ▼ - sixth heating to 750 °C; □ – seventh heating to 600 °C. Heating rate:  $20 \text{ }^\circ\text{C min}^{-1}$ .

Magnetic permeability was measured during heating. The as-deposited powder was heated to 360°C. Then it was cooled to 25 °C and reheated to 420 °C. Multiple heating and cooling runs were performed.

The diagrams in Fig. 5 show that magnetic permeability values are in agreement across the first four heating cycles, suggesting that heating to 500 °C does not cause irreversible structural changes. However, the magnetic permeability of the sample cooled after heating to 600°C is about 6% higher than that of the as-deposited powder. The cooled sample of the powder pre-heated to 650°C exhibits an increase of about 10% in magnetic permeability compared to the as-deposited powder.

The increase in the magnetic permeability of the powder cooled after annealing in the temperature range of 500°C to 650°C indicates that structural relaxation takes place in this temperature range. During structural relaxation, the alloy undergoes heat-induced structural short-range ordering. Owing to the higher energy obtained through heat, certain atoms cross the energy barrier and reach somewhat lower energy levels. At these lower levels, their 3d and 4s orbitals overlap to a higher extent with the same type of orbitals of neighboring atoms, thus contributing to an increase in both the exchange interval and the electronic density of states near the Fermi level [14-18,25-29]. At the same time, the mean length of the free electron path is increased [14-18,25-29]. The atoms translocated to lower energy levels attach to an energetically more favorable magnetic domain. The lower density of chaotically distributed dislocations formed during structural relaxation enables higher mobility of magnetic domain walls and facilitates their orientation in the external magnetic field [14-18,25-29]. These changes allow magnetic domain expansion and, hence, an increase in magnetic permeability.

The magnetic permeability of the powder annealed to 750°C and cooled to 25°C is about 33% lower than that of the as-deposited powder. The decrease in permeability is due to amorphous phase crystallization and FCC crystal grain growth. In the stable crystal structure, the orientation of certain magnetic domains is hampered and the mobility of the oriented domain walls is reduced.

Increasing the temperature of the as-deposited powder and the powders pre-annealed at temperatures below 650°C, in the temperature range of 280°C to 420°C, leads to an abrupt decrease in their magnetic permeability. A further increase in temperature in the temperature interval between 420°C and 620°C causes the magnetic permeability of the powders to decrease at a considerably lower rate.

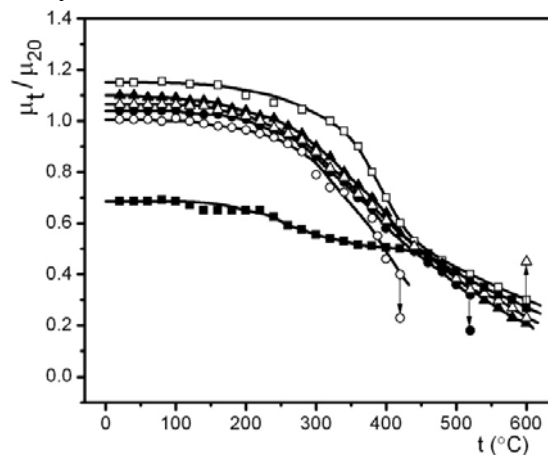


**Fig. 6.** Relative change in the magnetic permeability of the powder deposited at 800 mAcm<sup>-2</sup> as a function of temperature: o – first heating to 420°C; ● – second heating to 520°C; Δ - third heating to 600°C; ▲ – fourth heating to 650°C; □ – fifth heating to 750°C; ■- sixth heating to 650°C. Heating rate: 20 °C min<sup>-1</sup>.

At high electrodeposition current densities, clusters with different concentrations of nickel are formed in the amorphous phase. The orientation of the domains or part of the domains made up of clusters with a high nickel content is lost, due to heat, in the lower temperature interval (280°C-420°C). However, the magnetic domains made up of clusters rich in cobalt lose their orientation at higher temperatures (420°C-620°C).

Fig. 6. presents the temperature dependence of the relative magnetic permeability of the nickel-cobalt-molybdenum alloy powder electrodeposited at 800 mAcm<sup>-2</sup>.

The functions presented in Fig. 6. show that the structural relaxation of the powder obtained at 800 mAcm<sup>-2</sup> is initiated at a temperature 80°C lower than the starting temperature of relaxation for the powder obtained at 400 mAcm<sup>-2</sup>. This is due to the lower degree of short-range structural order of the powders obtained at higher current densities. At higher current densities, smaller FCC and HCP crystals and a less ordered amorphous phase with clusters having a lower average size, higher density of chaotically distributed dislocations and higher internal microstrains are formed [14-18,25-29].

The structural relaxation of the powder obtained at 800 mAcm<sup>-2</sup> causes an increase in its relative magnetic permeability at 25°C by about 14%. The crystallization of the powder at 750°C causes its relative magnetic permeability to decrease at room temperature to a value that is about 34% lower than the relative magnetic permeability of the as-deposited powder. The powder obtained at a current density of 1600 mAcm<sup>-2</sup> has the smallest FCC and HCP crystals and the highest content and the lowest degree of order of the amorphous phase containing clusters that are lowest in average size. Hence, the relaxation of this powder takes place at the lowest temperatures, with the powder exhibiting the highest increase in relative magnetic permeability during the structural relaxation (Fig. 7).

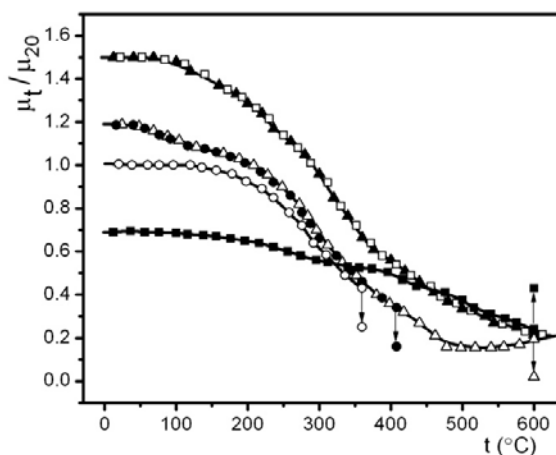


**Fig. 7.** Relative magnetic permeability of the powder deposited at 1600 mAcm<sup>-2</sup> as a function of temperature: o – first heating to 360°C; ● – second heating to 420 °C; Δ - third heating to 600°C; ▲ – fourth heating to 650°C; □ – fifth heating to 750 °C; ■- sixth heating to 600°C. Heating rate: 20°C min<sup>-1</sup>.

Structural relaxation occurs in the temperature range of 360°C to 600°C. The relative magnetic permeability of this structurally relaxed cooled powder is about 50% higher than that of the as-deposited powder. Heating the powder obtained at 1600 mAcm<sup>-2</sup> to 700°C causes a decrease in its relative magnetic permeability at 25°C to a value that is about 30% lower than that of the relative magnetic permeability of the as-deposited powder. The decrease is due to amorphous phase crystallization and FCC crystal grain growth.

The present results and the analysis thereof show an important effect of electrodeposition current density and annealing temperature for nickel-cobalt-molybdenum



alloy powders on their microstructure, and reveal a correlation between microstructure and magnetic properties. This suggests that the choice of electrodeposition current density and annealing temperature can help generate powders with pre-defined magnetic properties.

#### 4. Conclusion

Nickel-cobalt-molybdenum alloy powders were electrodeposited from an ammonium sulfate bath at current densities of 400, 800 and 1600 mAcm<sup>-2</sup>. The powders mostly consist of an amorphous phase and a small amount of nanocrystals of the FCC phase of the solid solution of cobalt and molybdenum in nickel and of the HCP phase of the solid solution of nickel and molybdenum in cobalt. Increasing current densities results in the formation of powders with smaller nanocrystals and a higher content of the amorphous phase showing a lower degree of order in the clusters, a lower average size, a higher density of chaotically distributed dislocations and higher internal microstrains.

The structural relaxation of the powders takes place at temperatures lower than 650°C. The structural relaxation of the powders exhibiting a lower degree of order is initiated at lower temperatures. The increase in relative magnetic permeability during structural relaxation is higher in the structurally less-ordered powders obtained at higher current densities. Annealing at 700°C causes crystallization and, hence, a decrease in the relative magnetic permeability of the powder.

#### Acknowledgments

This work was financially supported by the Ministry of Education and Science, Republic of Serbia, through Project No. 172057.

#### 5. References

1. P. Haasèn, R.J. Joffe, *Amorphous Metals and Semiconductors*, Pergamon, London, 1986.
2. H. Steerb, H. Warlimont, *Rapidly Quenched Metals*, Elsevier, Amsterdam, 1985.
3. P.L. Cavallotti, B. Bozzini, L. Nobili, G. Zangari, *Electrochim. Acta* 39 (1994) 1123
4. B. Löchel, A. Maciossek, *J. Electrochem. Soc.* 143 (1996) 3343.
5. Yu. A. Kunitsky, V.I. Lisov, T.L. Tsaregradskaya, O.V. Turkov, *Sci. Sinter.* 7 (2003) 319.
6. L.A. Jakobson, J. Mc. Kittrik, *Rapid Solidification Processing*, Elsevier, Amsterdam, 1994.
7. A.M. Maričić, M.M. Ristić, *Sci. Sinter.* 35 (2003) 31.
8. P. Elumalai, H.N.Vasan, M.Verelst, P. Lecante, V. Carles, P. Tailhades, *Mater. Res. Bull.* 37 (2002) 353.
9. L. Gunther, *Phys. World* 3 (1990) 28.
10. P. Toneguzzo, G. Viau, O. Acher, F. Fiévet-Vincent, F. Fiévet, *Adv. Mater.* 10 (1998) 1032.
11. F. Fievet, J. P. Lagier, M. Figlarz, *Mater. Res. Bull.* 14 (1989) 29.
12. K.V. P.M. Shafi, A. Gedenken, R. Prozorov, *J. Mater. Chem.* 8 (1998) 769.
13. Y.D. Li, L.Q. Li, H.W. Liao, H.R. Wang, *J. Mater. Chem.* 9 (1999) 2675.
14. A. Maričić, M. Spasojević, L. Rafailović, V. Milovanović, L. Ribić-Zelenović, *Mater. Sci. Forum* 45 (2004) 411.

15. L. Ribić-Zelenović, L. Rafailović, M. Spasojević, A. Maričić, Sci. Sinter. 38 (2006) 145.
16. L. Ribić-Zelenović, L. Rafailović, M. Spasojević, A. Maričić, Rhys. B Cond. Matter. 403 (2008) 2148.
17. S. Randjić, A. Maričić, L. Rafailović, M. Spasojević, M. Ristić, Sci. Sinter. 38 (2006) 139.
18. M. Spasojević, L. Ribić-Zelenović, A. Maričić, Sci. Sinter. 43 (2011) 313.
19. Daheum Kim, D. Y. Park, B.Y. Yoo, P.T.A. Sumodjo, N.V. Myung. Electrochim. Acta 48 (2003) 819.
20. N.V. Myung, K. Nobe, J. Electrochem. Soc. 148 (2001) C 136.
21. X.M. Liu, S.Y. Fu, C.J. Huang, Mater. Lett. 59 (2005) 3791.
22. C.A. Clark, Br. J. Appl. Phys. 7 (1956) 355.
23. K.V.P.M. Shafi, A. Gedanken, Ruslan Prozorov, J. Mater. Chem 8 (1998) 769.
24. E. Gómez, S. Pané, E. Vallés, Electrochim. Acta 51 (2005) 146.
25. L. Ribić-Zelenović, M. Spasojević, A. Maričić, M. Ristić, Sci. Sinter. 41 (2009) 175.
26. L. Ribić-Zelenović, M. Spasojević, A. Maričić, Mater. Chem. Phys. 115 (2009) 347.
27. L. Ribić-Zelenović, M. Spasojević, A. Maričić, M.M. Ristić, Sci. Sinter 41 (2009) 175.
28. L. Ribić-Zelenović, L. Rafailović, A. Maričić, M. Spasojević, J. Optoelectron. Advan. Mater. 9 (2007) 2681.
29. L. Ribić-Zelenović, M. Spasojević, A. Maričić, M. Ristić, J. Optoelectron. Adv. Mater. 10 (2008) 1384.
30. 30 A.R. Despić, K.I. Popov, Modern. Aspects of Electrochemistry, vol. 7, Plenum Press, New York, 1972.
31. M.A. Meyers, A. Mishada, D.J. Benson, Progress in Materials Science, 51 (2006) 427.
32. K.I. Popov, M.G. Pavlović, in: R.E. White, al, et (Eds.), Modern Aspects of Electrochemistry, Plenum Press, New York, 1993.
33. V.D. Jović, B.M. Jović, V. Maksimović, M.G. Pavlović, Electrochim Acta 52 (2007) 4254.
34. V.M. Maksimović, U.Č. Lačnjevac, M.M. Stoilković, M.G. Pavlović, V.D. Jović, Mater. Character. 62 (2011) 1173.
35. L.D. Rafailović, H.P. Karnthaler, T. Trišović, D.M. Minić, Mater. Chem. Phys. 120 (2010) 409.
36. M. Donten, H. Cesiulis, Z. Stojek, Electrochim. Acta 39 (2000) 3389.
37. D. Landolt, E.J. Podlaha, N. Zech, Zh. Phys. Chem. 2008 (1999) 167.
38. E.J. Podlaha, D. Landolt, J. Electrochem. Soc. 143 (1996) 893.
39. E.J. Podlaha, D. Landolt, J. Electrochem. Soc. 144 (1997) 1672.
40. 40 F. He, J. Yang, T. Lei, C. Gu, Appl. Surf. Sci. 253 (2007) 7591.
41. 41. S.J. Mun, T.H. Yim, J.Lee, T. Kang, J. Electrochem. Soc. 157 (2010) D 177.
42. 42. N. Mitrović, J. Magn. Mater. 262 (2003) 302.
43. 43. M. Donten, J. Solid State Electrochem. 3 (1999) 87.

---

**Садржај:** *Електродепозицијом из амонијачно-сулфатног купатила добијени су прахови наноструктурне легуре никла, кобалта и молибдена. Прахови се углавном састоје од аморфне фазе и врло мале количине нанокристала просечне димензије мање од 3 нм. Са порастом густине струје таложења у праховима се повећава удео аморфне фазе, густине хаотично распоређених дислокација и унутрашњих микронапрезања а опада просечна димензија нано кристала. Температурна област структурне релаксације*

---

*прахова депонованих на већим густинама струје је померена ка нижим температурама. Промена релативне магнетне пермеабилности током структурне релаксације је већа код прахова депонованим на већим густинама струје. Кристализација прахова одвија се на температурама вишим од 700 °C. Настанак стабилне кристалне структуре узрокује смањење релативне магнетне пермеабилности.*

**Кључне речи:** *рендгенска дифракција, наноструктурни материјали, дислокације, магнетна пермеабилност, прах.*

---